

## Micellization of Polyoxyalkylene Block Copolymers in Formamide

Paschalis Alexandridis\* and Lin Yang

Department of Chemical Engineering, University at Buffalo, The State University of New York, Buffalo, New York 14260-4200

Received June 1, 1999; Revised Manuscript Received February 14, 2000

**ABSTRACT:** The solution properties of amphiphilic molecules in nonaqueous polar solvents are important in the elucidation of the effects of solvent quality on self-assembly and also in practical applications where the use of water as a solvent is undesirable. We used small-angle neutron scattering (SANS) to investigate the micellization of a poly(ethylene oxide)–poly(propylene oxide)–poly(ethylene oxide) (PEO–PPO–PEO) block copolymer (Pluronic P105: EO<sub>37</sub>PO<sub>58</sub>EO<sub>37</sub>) in formamide as a function of block copolymer concentration (in the range 1–20 wt %) and temperature (10–60 °C). Results on the micellization thermodynamics and the micelle structure are presented here. PEO–PPO–PEO block copolymers self-assemble in formamide into micelles upon increasing the temperature, indicating an endothermic micellization. The enthalpy and entropy of micellization in formamide are about 3 times smaller than the respective quantities in water. The radius of gyration of the unimers and the core radius and hard-sphere interaction radius of the spherical micelles were obtained by fitting appropriate models to the SANS scattering patterns. The degree of swelling of the block copolymer micelles by the solvent was estimated on the basis of the different radii. The micelle radii and the corresponding number of block copolymers that participate in each micelle increase with increasing temperature. The amount of solvent in the micelle corona decreased with increasing temperature up to 15 °C above the critical micellization temperature and then remained constant (for the temperature range examined) at a value of about 1.5 solvent molecules per ethylene oxide segment.

## Introduction

Amphiphiles (molecules composed of parts having different chemical nature) find widespread applications because of their unique ability to self-assemble in solution and to modify interfacial and surface properties.<sup>1</sup> Surfactants are well-known to form micelles, thermodynamically stable assemblies of finite size and typically spherical shape, in aqueous solutions.<sup>2</sup> Block copolymers dissolved in selective solvents can also form micelles.<sup>3,4</sup> A class of block copolymers that have attracted considerable attention over the recent years because of their self-assembly properties in aqueous solutions are the Poloxamers or Pluronics that are composed of water-soluble poly(ethylene oxide) (PEO) blocks and water-insoluble poly(propylene oxide) (PPO) blocks.<sup>5,6</sup>

The versatility, in terms of self-assembly and corresponding practical applications, of the PEO–PPO block copolymers emanates from (i) the broad and controllable range of amphiphilic properties achieved by the variation of the PPO/PEO ratio and the block copolymer molecular weight and (ii) the sensitivity of their aqueous solution properties to the temperature.<sup>6</sup> PEO–PPO block copolymers in aqueous solutions can self-assemble into spherical micelles (with a PPO core and a hydrated PEO corona), above a certain polymer concentration, cmc (critical micellization concentration), and/or above a certain solution temperature, cmt (critical micellization temperature), which depend on the PEO/PPO block ratio and the polymer molecular weight.<sup>7,8</sup> The formation of thermoreversible “gels” in water is a notable self-assembly feature of PEO–PPO block copolymers. Such gels have been known for long time and utilized in, e.g., controlled release,<sup>9,10</sup> but their structure has only

recently been identified as lyotropic liquid crystalline.<sup>6,8,11,12</sup> In ternary systems with water (selective solvent for PEO) and an organic solvent (such as xylene) selective for PPO, PEO–PPO block copolymers can form the whole spectrum of self-assembled structures, from micellar solutions in water, to lyotropic liquid crystals of “oil-in-water” or “water-in-oil” topology, to water-swollen “reverse” micellar solutions.<sup>13–15</sup> The micellar solutions possess only short-range order (at the micelle level). The lyotropic liquid crystals exhibit long-range order beyond the level of the structural element (i.e., spherical, cylindrical, or planar block copolymer micelles).

The properties (“quality”) of the solvent is a controlling factor in the self-assembly of amphiphiles. The solvent quality of water toward PPO and PEO can be altered by a change in temperature<sup>7</sup> or by the addition of cosolutes such as alcohols,<sup>16</sup> urea,<sup>17</sup> or salts.<sup>18</sup> However, for some applications it is desirable to replace water completely by a nonaqueous polar solvent.<sup>19</sup> Moreover, the elucidation of the phase behavior and structure of amphiphiles in nonaqueous solvents is important for the description of the “hydrophobic effect” which is considered responsible for the self-assembly of amphiphiles in water.<sup>20</sup> These considerations have prompted a number of studies on the solution behavior of surfactants in a variety of nonaqueous polar solvents such as hydrazine, formamide, *N*-methylformamide, glycerol, propylene glycol, and ethylene glycol.<sup>21,22</sup> Formamide (HCONH<sub>2</sub>) has been the solvent studied most extensively in this context.<sup>23–28</sup> Nonionic PEO–alkyl ether surfactants have been found to form micelles and even lyotropic liquid crystalline structures in formamide, but over different conditions than in water.<sup>23–25</sup> Cloud point (macrophase separation) measurements for a PEO–PPO block copolymer in formamide have been made,<sup>29</sup> and a report on the synthesis of ordered

\* To whom correspondence should be addressed. Fax (716) 645 3822; e-mail palexand@eng.buffalo.edu.

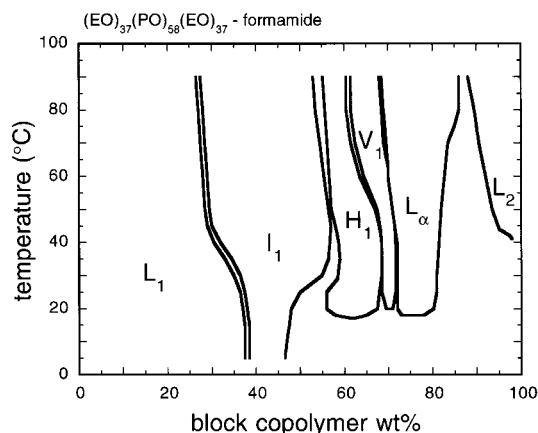


**Figure 1.** Concentration-temperature phase diagram of the  $\text{EO}_{37}\text{PO}_{58}\text{EO}_{37}$ -formamide ( $\text{HCONH}_2$ ) binary system. The phase boundaries of the one-phase regions are drawn with solid lines. The samples whose compositions fall outside the one-phase regions are dispersions of two different phases.  $I_1$ ,  $H_1$ ,  $V_1$ , and  $L_\alpha$  denote micellar cubic, hexagonal (cylindrical), bicontinuous cubic, and lamellar (smectic) lyotropic liquid crystalline phases, respectively, while  $L_1$  and  $L_2$  denote formamide-rich and polymer-rich solutions (adapted from ref 31).

macroporous materials by templating with oil-in-formamide emulsions stabilized by PEO-PPO-PEO block copolymers has appeared.<sup>30</sup>

We recently reported<sup>31</sup> the phase behavior and structure in formamide of a PEO-PPO block copolymer with known aqueous self-assembly properties.<sup>12,32</sup> We found that lyotropic liquid crystals with a variety of morphologies can be formed in formamide, and we identified the concentration-temperature "window" where a heat-induced transition from a micellar solution to a micellar cubic crystal occurs (see Figure 1).<sup>31</sup> Here we focus our attention on the formamide-rich solution region of the binary phase diagram and present results on the cmc and cmt, thermodynamic parameters of micellization, and micelle structure (i.e., micelle radius, association number, and degree of solvation), obtained from extensive small-angle neutron scattering (SANS) experiments. To the best of our knowledge, this is first report on the micellization of PEO-PPO block copolymers in nonaqueous polar solvents. In conjunction with the knowledge of phase behavior,<sup>31</sup> the information presented here provides a comprehensive picture of the self-assembly of PEO-PPO-PEO block copolymers in formamide, as a representative nonaqueous polar solvent. Moreover, this is a case study on solvent quality effects on block copolymer micelle formation and structure which transcends the specific case of PEO-PPO block copolymers.

## Materials and Methods

**Materials.** The Pluronic P105 poly(ethylene oxide)-*block*-poly(propylene oxide)-*block*-poly(ethylene oxide) copolymer was obtained as a gift from BASF Corp. and was used as received. Pluronic P105 is represented here by the formula  $\text{EO}_{37}\text{PO}_{58}\text{EO}_{37}$  on the basis of its nominal molecular weight of 6500 and 50% PEO content. Deuterated formamide ( $\text{DCOND}_2$ ) was purchased from Cambridge Isotope Laboratories. Care was taken to avoid exposure of formamide to atmospheric humidity.

**Phase Behavior of the  $\text{EO}_{37}\text{PO}_{58}\text{EO}_{37}$ -Formamide System.** The concentration-temperature phase diagram for the binary  $\text{EO}_{37}\text{PO}_{58}\text{EO}_{37}$ -formamide ( $\text{HCONH}_2$ ) system is presented in Figure 1. A total of six different one-phase regions have been identified: four regions with lyotropic liquid crystalline structure, micellar cubic ( $I_1$ ), hexagonal (cylindrical) ( $H_1$ ),

bicontinuous cubic ( $V_1$ ), and lamellar ( $L_\alpha$ ), and two isotropic solution phases, one rich in formamide ( $L_1$ ) and one rich in polymer ( $L_2$ ). The block copolymer we studied is "symmetric", having 50% PEO and 50% PPO content, and in the absence of solvent (more accurately, in the presence of sufficient solvent to solvate the crystalline PEO segments) it prefers the lamellar ( $L_\alpha$ ) arrangement. As the amount of solvent increases (and the concentration of block copolymer decreases—from right to left in Figure 1), the solvated PEO blocks occupy progressively more volume than the PPO blocks, thus leading to the formation of cylinders ( $H_1$ ) and spheres ( $I_1$ ), morphologies which enclose PPO-rich domains and allow more "room" for the solvated PEO blocks. Below a certain block copolymer concentration, the ordered structures are no longer stable and revert to a disordered solution ( $L_1$ ). As seen in Figure 1, the structural polymorphism of the PEO-PPO block copolymer is not diminished by having formamide as a selective solvent instead of water. Still, the stability regions of the nonlamellar structures (and in particular of the micellar cubic  $I_1$ ) are shifted to higher polymer concentrations and temperatures in the case of formamide compared to water.<sup>31</sup> The phase diagram of Figure 1 forms the background of the present study. Here we concentrate on the microstructure in the  $L_1$  solution region. The extensive  $I_1$  micellar cubic gel region, with a "window" of thermoreversible liquid-to-gel transition, is an interesting feature of the  $\text{EO}_{37}\text{PO}_{58}\text{EO}_{37}$ -formamide phase diagram, which points to the importance of temperature in the self-assembly. Accordingly, temperature has been an important variable in the present study. The transition from a Newtonian liquid (micellar solution) to a soft solid material ("gel") occurs in aqueous PEO-PPO copolymer solutions when the micellar volume fraction crosses the critical value for hard-sphere crystallization, for sufficiently repulsive intermicellar interactions.<sup>8</sup>

**Small-Angle Neutron Scattering (SANS).** SANS measurements were performed at the National Institute of Standards and Technology (NIST) Center for Neutron Research (NCNR), beam guide NG3. The neutron wavelength used was  $\lambda = 0.6$  nm. The sample-to-detector distance was 260.0 cm. The resolution ( $\Delta q/q$ ) was about 0.15. The angular distribution of the scattered neutrons was recorded in a two-dimensional detector; the radial average was subsequently obtained and used for data analysis. The PEO-PPO block copolymer solutions in deuterated formamide (concentrations: 0, 1, 3, 8, 15, and 20 wt %) were placed in stoppered 1 mm path length "banjo" quartz cells, and scattering data were recorded at different temperatures in the range 10–60 °C. Adequate time was allotted for thermal and kinetic<sup>33</sup> equilibration. Scattering intensities from the block copolymer solutions were corrected for detector background, empty cell scattering, and sample transmission. SANS is a very powerful tool for the study of hydrogenated block copolymers in deuterated solvents.<sup>34</sup> SANS has proven a very useful tool in the study of the micelle structure in aqueous solutions of PEO-PPO block copolymers.<sup>35–40</sup> Furthermore, SANS studies on shear-aligned PEO-PPO block copolymer-water lyotropic liquid crystalline samples have been instrumental in the elucidation of their microstructure.<sup>41–46</sup>

## Results and Discussion

**Concentration and Temperature Dependence of Scattering Patterns.** The evolution of the scattering function as a function of block copolymer concentration and solution temperature is indicated in the representative scattering patterns from  $\text{EO}_{37}\text{PO}_{58}\text{EO}_{37}$ -formamide shown in Figures 2 and 3. A wide block copolymer concentration range (1–20%) and solution temperature range (10–60 °C) was covered. Two different regimes are evident from such scattering curves: (i) at low concentrations (e.g., 1–8%) and low temperatures (e.g., 10–20 °C) the scattering functions show relatively weak  $q$  dependence and only low intensities, indicating scattering from individual block copolymers, which are

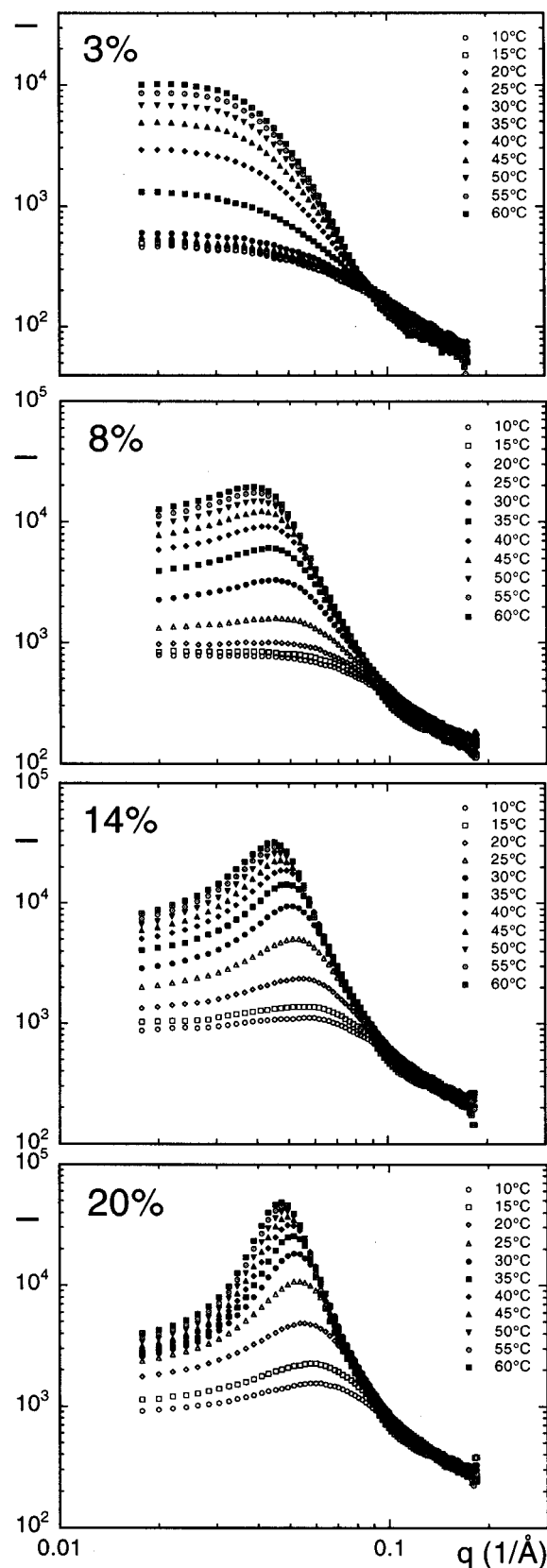


**Figure 2.** Representative SANS scattering patterns from EO<sub>37</sub>PO<sub>58</sub>EO<sub>37</sub>-formamide (DCOND<sub>2</sub>) solutions as a function of temperature (10, 15, 20, 25, 30, 35, 40, 45, 50, 55, and 60 °C) for a given block copolymer concentration: from top to bottom, 3, 8, 14, and 20 wt %.

denoted here as unimers; (ii) at higher temperatures the intensity increases, reflecting the association of unimers into micelles, while at high concentrations (14–18%)

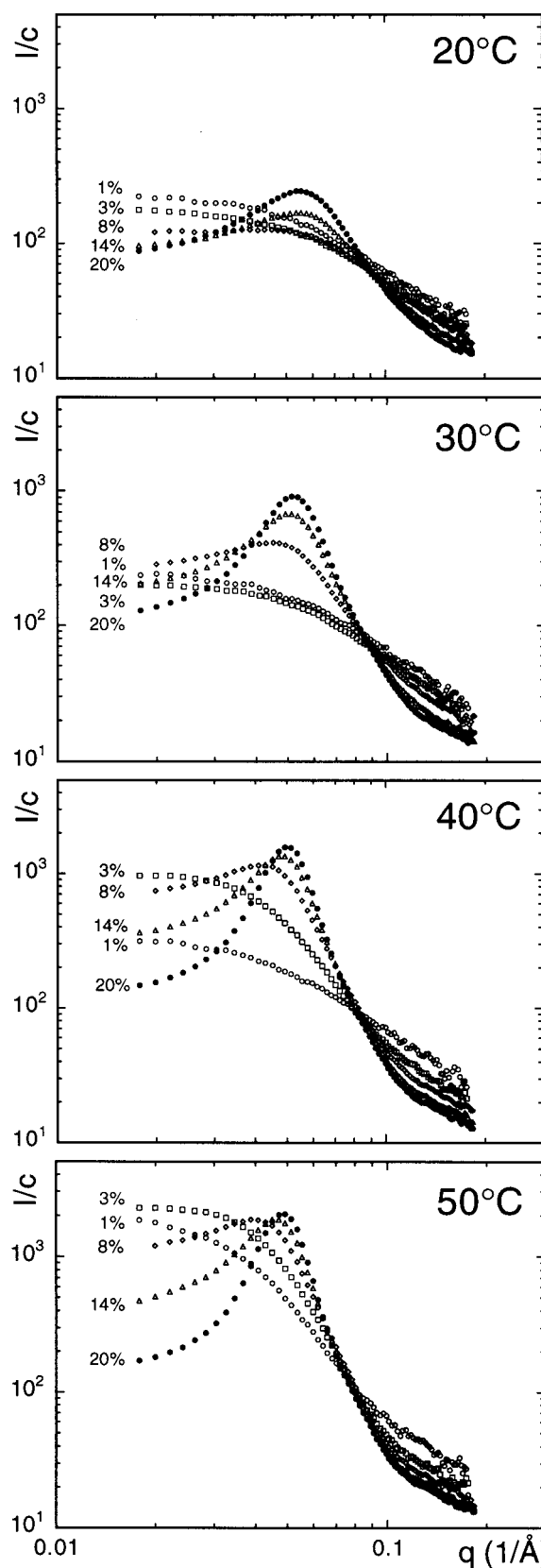


**Figure 3.** Representative SANS scattering patterns from EO<sub>37</sub>PO<sub>58</sub>EO<sub>37</sub>-formamide (DCOND<sub>2</sub>) solutions of different block copolymer concentrations (1, 3, 8, 14, and 20 wt %) at the same temperature: from top to bottom, 20, 30, 40, and 50 °C. The scattering intensity has been normalized with respect to the block copolymer concentration.

and temperatures (30–60 °C) the scattering function is dominated by a pronounced correlation peak which

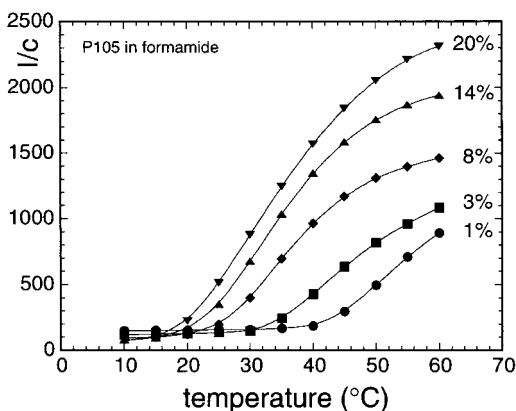


**Figure 4.** Scattering intensity ( $I/c$ ) at  $q = 0.05 \text{ \AA}^{-1}$ , normalized with respect to the block copolymer concentration, plotted as a function of temperature for  $\text{EO}_{37}\text{PO}_{58}\text{EO}_{37}$ –formamide ( $\text{DCOND}_2$ ) solutions of different block copolymer concentrations (1, 3, 8, 14, and 20 wt %). Note that at low temperatures  $I/c$  is the same for all block copolymer concentrations examined. The increase of  $I/c$  with increasing temperature is indicative of the formation of micelles.

originates from intermicellar interactions. Note that in Figure 2, where the scattering intensities are plotted for different temperatures at a fixed concentration, the high- $q$  scattering intensity, which originates from the block copolymer segments, is not affected by the temperature. Also, when the scattering intensities plotted for different concentrations and a fixed temperature are normalized with respect to the block copolymer volume fraction (see Figure 3), then the high- $q$  part becomes similar for all concentrations. Information about the structure of the unimers or micelles, but also about the onset of micellization, can be extracted from the scattering patterns, as discussed below. First we examine the micelle formation and then continue with the micelle structure.

**Micellization Boundary.** The formation of micelles in an aqueous amphiphile solution, upon an increase in the amphiphile concentration, is reflected in a number of properties such as surface tension or electrical conductivity in the case of ionic surfactants.<sup>1,2</sup> The sensitivity of the PEO–PPO block copolymer micellization on temperature allows the utilization of other methods for the determination of the temperature where micelles start forming at a given concentration, cmt. The micellization transition can be observed, for example, in an endothermic peak detected by differential scanning calorimetry,<sup>18</sup> in the enhanced solubilization of hydrophobic species detected by fluorescence,<sup>32</sup> or in an increase of the light scattering intensity.<sup>32</sup> In a study of PEO–PPO block copolymer micellization in water, we found the results from different techniques to be in very good agreement, provided the different data were analyzed in a consistent manner.<sup>32</sup> In fact, we found that the use of the same sample (fixed concentration) at different temperatures for the determination of cmt–cmt has advantages over the use of a series of samples of different concentration at a fixed temperature. Here we analyzed the temperature dependence of the neutron scattering intensity data, normalized with respect to the block copolymer concentration (shown in Figure 3), to obtain the cmt values for different PEO–PPO block copolymer concentrations in formamide.

Figure 4 shows the normalized scattering intensity ( $I/c$ ) at  $q = 0.05 \text{ \AA}^{-1}$  plotted as a function of temperature for  $\text{EO}_{37}\text{PO}_{58}\text{EO}_{37}$ –formamide solutions of different

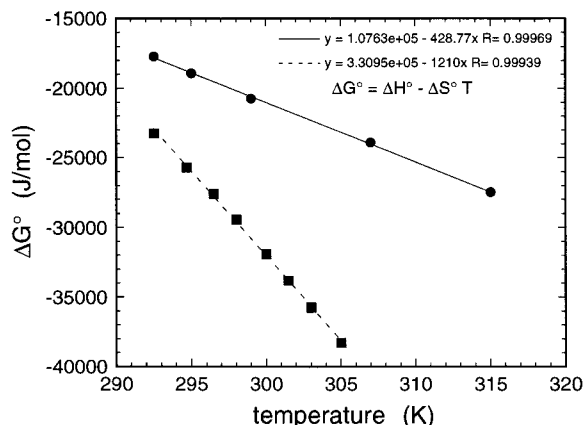
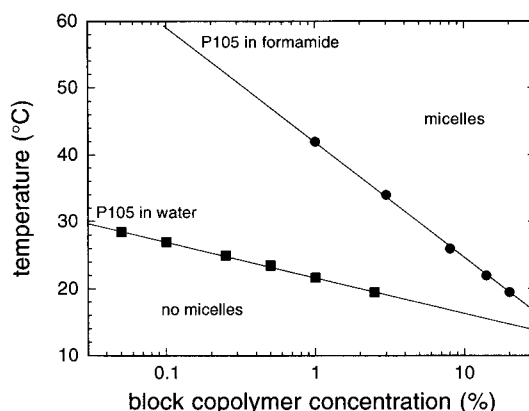


**Figure 5.** (top) Micellization boundary for  $\text{EO}_{37}\text{PO}_{58}\text{EO}_{37}$  dissolved in formamide ( $\text{DCOND}_2$ ). Also shown in the same plot, for comparison reasons, is the micellization boundary for  $\text{EO}_{37}\text{PO}_{58}\text{EO}_{37}$  dissolved in water ( $\text{H}_2\text{O}$ ). The micellization boundary represents cmt and cmc data. At temperatures and concentrations below the micellization boundary, the block copolymers do not associate (unimers). At temperatures and concentrations above the micellization boundary, micelles are formed which coexist in equilibrium with unimers. (bottom) Free energy of micelle formation,  $\Delta G^\circ$ , plotted as a function of temperature for the  $\text{EO}_{37}\text{PO}_{58}\text{EO}_{37}$ –formamide and  $\text{EO}_{37}\text{PO}_{58}\text{EO}_{37}$ –water systems. The linear fits shown in the inset lead to the estimation of the enthalpy  $\Delta H^\circ$  and entropy  $\Delta S^\circ$  of micellization.

block copolymer concentrations (1, 3, 8, 14, and 20 wt %).  $q = 0.05 \text{ \AA}^{-1}$  has been selected because it corresponds to the micelle correlation peak, as seen in Figures 2 and 3. (Note that the  $q$  value of the maximum position at the correlation peak changes with temperature, but we selected an average, fixed  $q$  in obtaining the data of Figure 4.) At low temperatures and concentrations the scattering intensity  $I/c$  is similar for all concentrations and does not vary with temperature. For each block copolymer concentration, there is a characteristic temperature, whereupon a further temperature increase,  $I/c$  increases, indicating the formation of micelles. We defined the cmt from the intercept of the horizontal line passing through the temperature-independent  $I/c$  data points and of the tangent to the increasing  $I/c$ . The cmt values are plotted in Figure 5 for the corresponding block copolymer concentrations. The line connecting the cmt–cmc points can be viewed as a micellization boundary within the  $L_1$  solution region of the phase diagram of Figure 1. At temperatures and concentrations below the micellization boundary, the block copolymers do not associate (unimers). At temperatures and concentrations above the micellization boundary, micelles are formed which coexist in



equilibrium with unimers. (The unimer concentration in equilibrium with micelles decreases rapidly with increasing temperature and eventually becomes vanishingly small.<sup>18</sup>)

Also shown in the same plot (Figure 5) for comparison reasons is the micellization boundary for EO<sub>37</sub>PO<sub>58</sub>EO<sub>37</sub> dissolved in water (H<sub>2</sub>O). Note that for a given temperature EO<sub>37</sub>PO<sub>58</sub>EO<sub>37</sub> forms micelles in water at a much lower concentration than in formamide; for example, the cmc in formamide at 25 °C is more than 2 orders of magnitude higher than the cmc in water. A similar trend has been reported in nonionic surfactants (short "block copolymers") of the C<sub>*n*</sub>E<sub>*m*</sub> type (where *n* = alkyl chain carbon number and *m* = number of ethylene oxide groups). According to ref 23, the cmc's of C<sub>12</sub>E<sub>6</sub> and C<sub>14</sub>E<sub>6</sub> in formamide are about 200 times larger than in water, whereas according to ref 25, the cmc's of C<sub>12</sub>E<sub>4</sub>, C<sub>12</sub>E<sub>6</sub>, and C<sub>16</sub>E<sub>8</sub> are a 1000-fold higher in formamide than in water. (Note that there is some inconsistency between the cmc values reported in refs 23 and 25 because of the different methods used to detect the cmc.)

**Thermodynamics of Micellization in Formamide.** The temperature dependence of the cmc in surfactant solutions can be analyzed in order to provide information on the thermodynamics parameters of micellization.<sup>7</sup> The standard free energy change for the transfer of 1 mol of amphiphile from solution to the micellar phase (free energy of micellization), Δ*G*<sup>°</sup>, assuming an equilibrium between unimer and micelles, is given by

$$\Delta G^{\circ} = RT \ln(X_{\text{cmc}}) \quad (1)$$

where *R* is the ideal gas law constant, *T* is the absolute temperature, and *X*<sub>cmc</sub> is the critical micellization concentration, expressed in mole fraction units, at temperature *T*. (cmc values at different temperatures can be obtained from the micellization boundary of Figure 5.) Δ*G*<sup>°</sup> is expressed in terms of the standard enthalpy of micellization, Δ*H*<sup>°</sup>, and the standard entropy of micellization per mole of surfactant, Δ*S*<sup>°</sup>, as

$$\Delta G^{\circ} = \Delta H^{\circ} - T\Delta S^{\circ} \quad (2)$$

The micellization free energy values, Δ*G*<sup>°</sup>, are negative since thermodynamically stable micelles are formed spontaneously. Furthermore, Δ*G*<sup>°</sup> becomes more negative at higher temperatures, indicating a larger driving force for micellization. The standard enthalpy of micellization, Δ*H*<sup>°</sup>, can be calculated from the intercept of a linear fit of the Δ*G*<sup>°</sup> vs *T* data (see Figure 5), in accordance with eq 2, provided that Δ*H*<sup>°</sup> is independent of temperature. The Δ*H*<sup>°</sup> value thus obtained for EO<sub>37</sub>PO<sub>58</sub>EO<sub>37</sub> in formamide, 108 kJ/mol (compared to 331 kJ/mol in water),<sup>7</sup> is positive, indicating that the transfer of the block copolymer molecules from the formamide solution to the micelle is an enthalpically disfavored endothermic process. Thus, a positive entropy contribution must be the driving force for the micellization: the association of the block copolymers, while it decreases the entropy of the individual block copolymer chains (since they order locally in the micelles) still leads to an increase of the overall solution enthalpy.<sup>5,7</sup> The positive entropy contribution has been related to an entropy gain by the solvent molecules when the PEO–PPO block copolymers associate and/or to a decrease in the polarity of the EO and PO segments with increasing temperature.<sup>5,7</sup> Entropy-driven micellization

is a common phenomenon in aqueous surfactant solutions, but not in block copolymers dissolved in apolar solvents.<sup>3,15</sup> In the latter case, the micellization is usually exothermic, and the system entropy decreases upon micellization.

Replacement of water by formamide alters significantly the magnitude of Δ*H*<sup>°</sup> (from 331 to 108 kJ/mol) but does not affect the fundamental mechanism (entropic driving force) responsible for the PEO–PPO block copolymer micellization. The entropy of EO<sub>37</sub>PO<sub>58</sub>EO<sub>37</sub> micellization in formamide is 0.43 kJ/(mol K), also much smaller than the corresponding value measured<sup>7</sup> in water, 1.21 kJ/(mol K). The relative changes in both Δ*H*<sup>°</sup> and Δ*S*<sup>°</sup> have the same magnitude, ≈65% decrease from water to formamide. The cmc values for C<sub>*n*</sub>E<sub>*m*</sub> surfactants in formamide yield a free energy increment per CH<sub>2</sub> of Δ*G*<sup>°</sup>(CH<sub>2</sub>) = −1.36 kJ/mol for the transfer from the solution phase to the micelle pseudo-phase, as compared to −3.3 kJ/mol in water, at 25 °C.<sup>23</sup> This decrease (by ≈58%) is comparable to the ≈65% decrease observed for PEO–PPO block copolymers.

The dependence of the micellization enthalpy on the block copolymer molecular weight and block composition has been reported for a number of PEO–PPO block copolymers in water.<sup>5,7</sup> The lowest Δ*H*<sup>°</sup> and Δ*S*<sup>°</sup> values observed for PEO–PPO micellization in water (out of 12 different PEO–PPO block copolymers examined) were 168 kJ/mol and 0.638 kJ/(mol K), respectively.<sup>7</sup> These values were obtained for Pluronic F88, which has a higher PEO content (80%) and is thus more hydrophilic in water than the Pluronic P105 (EO<sub>37</sub>PO<sub>58</sub>EO<sub>37</sub>) which we study here. EO<sub>37</sub>PO<sub>58</sub>EO<sub>37</sub> appears thus to be much more "solvophilic" (less "solvophobic") in formamide than it is in water. This is consistent with the effects of formamide on the PEO–PPO block copolymer conformation discussed in the following section.

A note about the closed association model used above in the estimation of Δ*H*<sup>°</sup> and Δ*S*<sup>°</sup>: this model assumes the micelle association number (number of block copolymers in one micelle) to be independent of temperature. As discussed below, from the analysis of the SANS data we obtain an association number which increases with temperature. This inconsistency, however, does not affect much the Δ*H*<sup>°</sup> and Δ*S*<sup>°</sup> values because the unimer-to-micelle association is still closed and not open. Moreover, as shown in Figure 5, the data fit well the linear relationship Δ*G*<sup>°</sup> = Δ*H*<sup>°</sup> − *T*Δ*S*<sup>°</sup>. Finally, the Δ*H*<sup>°</sup> and Δ*S*<sup>°</sup> we obtained for formamide are being compared to values for water that have been obtained assuming the closed association model to be valid.

**Effect of Formamide on the PEO–PPO–PEO Block Copolymer Self-Assembly.** The extent of the solvent interaction with polar headgroups, in particular with poly(ethylene oxide) segments of nonionic surfactants, and of the solvent penetration into surfactant assemblies is sometimes a controversial issue that affects the interpretation of data in surfactant solutions.<sup>22</sup> At the same time, the possibilities of tuning the interactions with a new parameter, i.e., the properties of the polar solvent, should be beneficial to industrially relevant applications, e.g., in the case of formulations of water-insoluble compounds, where the use of a nonaqueous polar solvent may increase the amount of water-insoluble compounds that can be loaded in the formulation.<sup>47</sup> The pronounced increase in the cmc–cmt, and the corresponding decrease in the enthalpy Δ*H*<sup>°</sup> and entropy Δ*S*<sup>°</sup> of micellization, observed in the PEO–PPO

block copolymer–formamide solution examined here, compared to the aqueous solution of the same PEO–PPO block copolymer, is reminiscent of the effects that salts and cosolutes such as NaI and urea have, when added to water, on the micellization of amphiphiles. For example, 4 M urea (about 25 wt % in water) decreased the micellization enthalpy of EO<sub>37</sub>PO<sub>58</sub>EO<sub>37</sub> from 331 to 230 kJ/mol,<sup>17</sup> not as low as in formamide solutions (108 kJ/mol) but still a significant decrease. NaI (2 M) decreased  $\Delta H^\circ$  in the case of EO<sub>13</sub>PO<sub>30</sub>EO<sub>13</sub> (Pluronic L64) by about 8%.<sup>18</sup> In the same system, 2 M NaCl increased  $\Delta H^\circ$  by about 35%.<sup>18</sup> The effects of salts and cosolutes in the micellization of surfactants in aqueous solutions are often described in terms of (i) an indirect mechanism, whereby the cosolutes affect (“structure-breaking” or “structure-making”) the water hydrogen bonding structure, or (ii) a direct mechanism where the cosolutes do not affect the water structure but replace water molecules from the hydration shell of the surfactant.<sup>18</sup> According to this terminology, formamide has less “structure” than water and/or enhances the solvation of the amphiphile compared to the case of water. Such enhanced solvation is being revealed by our SANS measurements as discussed in the following section.

An enhanced solvation of the PEO–PPO block copolymer in formamide is also reflected in the concentration–temperature phase diagram of Figure 1. The stability regions of the different structures (and in particular of the micellar cubic, I<sub>1</sub>) are shifted to higher polymer concentrations and temperatures in the case of formamide compared to the case of water.<sup>31</sup> Inspection of the phase diagram, together with the values for characteristic lengths of the lyotropic microstructures obtained from small-angle X-ray scattering (the lattice parameters in formamide are lower than those in water, and the interfacial areas per block copolymer in formamide are higher than those in water), indicates that formamide “swells” the PEO blocks 10–30% more than water does.<sup>31</sup> These observations have been related to a higher solubility of both PEO and PPO in formamide compared to the case of water and/or to a higher effective PEO/PPO block ratio of the polymers.<sup>31</sup> Formamide is considered a better solvent than water for the PEO–PPO block copolymer, and the degree of segregation between PEO and PPO blocks is weaker. The formation in the presence of formamide of a relatively extensive region of bicontinuous structure (V<sub>1</sub>) is also indicative of such weak segregation.<sup>31</sup>

**SANS Data Analysis: Unimer Radius.** At low temperature and concentration, the block copolymers occur in solution as independent polymer chains (unimers). Within statistical error (see Figure 6a), the scattering function of these unimers is in agreement with that of polymers obeying a Gaussian conformation (Debye function for the form factor of random coils):<sup>8</sup>

$$F_{\text{coil}}(q) \sim x^{-2}[\exp(-x) + x - 1] \quad (3)$$

where  $x = (qR_g)^2$ , and  $R_g$  is the polymer chain radius of gyration. The radii of gyration values resulting from the best fit of the scattering patterns to the Debye function (see Figure 6a for representative fits) are plotted in Figure 7a. The unimer  $R_g$  appears independent of concentration (for the 1 and 3% concentrations examined) and approximately constant to 28 Å with increasing temperature. (A small increase in  $R_g$  upon approach of the cmc–cmt boundary may be due to contributions

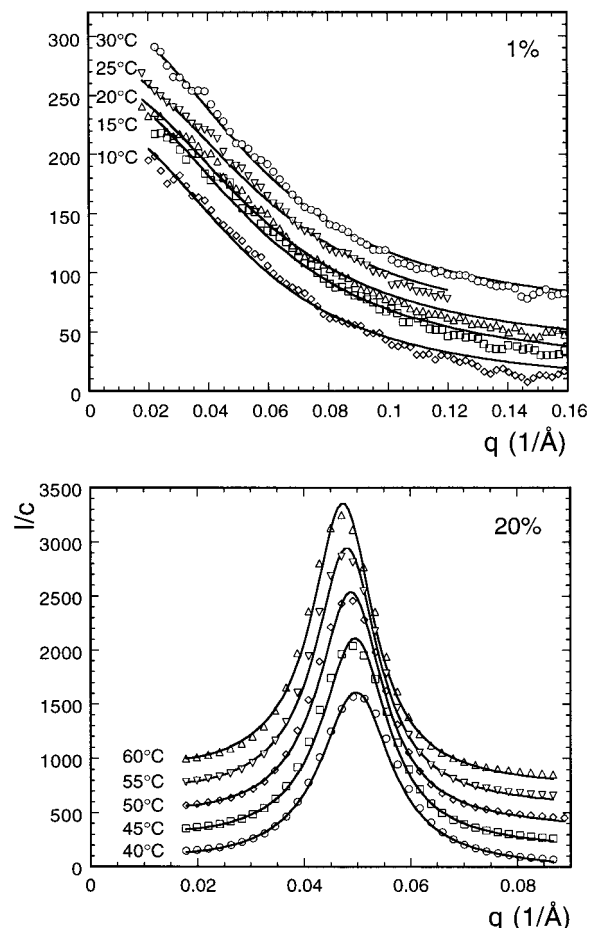


**Figure 6.** Representative examples of fits of the models (discussed in the text) to the SANS data, used to extract in formation on the (top) unimer and (bottom) micelle radii. The block copolymer concentration and temperature are indicated in the graphs.

from premicellar aggregates.) This value ( $R_g = 28$  Å) is greater than the  $R_g = 19$  Å expected (from an interpolation of data reported in ref 8) for the same PEO–PPO block copolymer in water, indicating better solvent conditions in formamide than in water.

**SANS Data Analysis: Micelle Radii.** With increasing temperature, the solvent conditions become progressively worse, leading to the association of unimers into spherical micelles. In aqueous solutions it is well accepted that these micelles are each composed of a core dominated by PPO blocks and surrounded by a corona of hydrated PEO segments. Model calculations<sup>48</sup> have described the micelle structure adequately. The scattering function of EO<sub>37</sub>PO<sub>58</sub>EO<sub>37</sub>–formamide solutions at high temperatures and/or concentrations clearly shows a side maximum as expected from the form factor of dense spherical objects with sharp interfaces and a radius  $R_c$ .<sup>8</sup>

$$F_c(q) \sim \{3y^{-3}[\sin(y) - y \cos(y)]\}^2 \quad (4)$$

where  $y = qR_c$ .  $R_c$  corresponds to the core of the block copolymer micelle, where the contrast between the hydrogenated block copolymer segments and the deuterated solvent is the maximum. If we assume that the micelle core consists of all the PPO blocks (and only PPO blocks), then we can use  $R_c$  to obtain the amount of PPO per micelle and, from this, the number of block copolymer molecules per micelle,  $N_{\text{association}}$  (see next section).

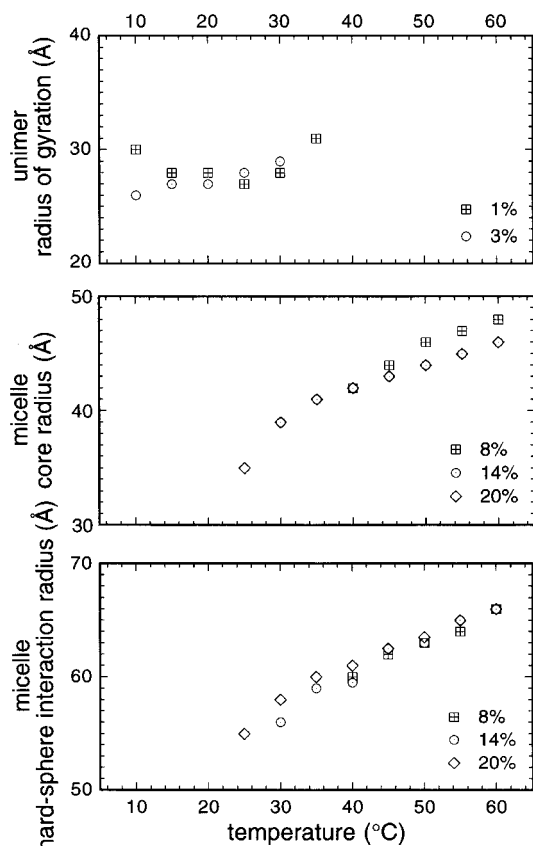


**Figure 7.** Structural information obtained from SANS in EO<sub>37</sub>PO<sub>58</sub>EO<sub>37</sub>-formamide (DCOND<sub>2</sub>) solutions, plotted as a function of temperature: (top) unimer radius of gyration for low (1 and 3 wt %) block copolymer concentrations, (middle) micelle core radius for high (8, 14, and 20 wt %) block copolymer concentrations, and (bottom) micelle hard-sphere interaction radius for high (8, 14, and 20 wt %) block copolymer concentrations.

At large  $q$  values the experimental form factor shows a  $q^{-2}$  dependence rather than the  $q^{-4}$  expected from the form factor of a hard sphere (eq 4). This deviation has also been observed in PEO-PPO block copolymers in water and has been attributed to the presence of solvated PEO segments (which behave as Gaussian chains in eq 3) either in the micelle corona or in solution.<sup>8</sup> The scattering intensity at high  $q$  decreases with increasing temperature (at a fixed total block copolymer concentration), suggesting that the concentration of Gaussian chains decreases as the unimer-to-micelle equilibrium is shifted to favor micelles.

A significant reduction in the scattering intensity is observed at low  $q$  with increasing block copolymer concentration. This reduction is a result of intermicellar interactions, and it constitutes a warning that the form factor of eq 4 is not an adequate description of the scattering patterns. If we assume a monodisperse solution of micelles, then the scattering function can be written as a product of the single-particle form factor,  $F(q)$ , and a structure factor,  $S(q)$ , which depends on the spatial distribution of the micelles and describes the interparticle interference:<sup>8</sup>

$$I(q) = \Delta\rho^2 N F(q) S(q) \quad (5)$$

where  $\Delta\rho$  is the contrast factor and  $N$  is the number density of the micelles. Using the classical Ornstein-Zernike approximation for the spatial correlation func-

tions and the Percus-Yevick approximation for describing the direct correlation between two scattering objects with hard-sphere nearest-neighbor interacting potential, the structure factor can be written in the analytical form:<sup>8,39</sup>

$$S(q) = [1 + 24\phi G(2qR_{hs})/(2qR_{hs})]^{-1} \quad (6)$$

where  $\phi$  is the micellar volume fraction ( $\phi = C4\pi R_{hs}^3/3N_{\text{association}}$ , with  $C$  being the weight percent block copolymer concentration),  $R_{hs}$  is the hard-sphere interaction distance, and  $G$  is a trigonometric function of  $z = 2qR_{hs}$  and  $\phi$ :<sup>8</sup>

$$G(z, \phi) = [\alpha(\phi)/z^2][\sin(z) - z \cos(z)] + [\beta(\phi)/z^3][2z \sin(z) + (2 - z^2) \cos(z) - 2] + [\gamma(\phi)/z^5]\{-z^4 \cos(z) + 4[(3z^3 - 6) \cos(z) + (z^3 - 6z) \sin(z) + 6]\} \quad (7)$$

where  $\alpha$ ,  $\beta$ , and  $\gamma$  are defined as

$$\begin{aligned} \alpha &= (1 + 2\phi)^2/(1 - \phi)^4 \\ \beta &= -6\phi(1 + \phi/2)^2/(1 - \phi)^4 \\ \gamma &= (\phi/2)(1 + 2\phi)^2/(1 - \phi)^4 \end{aligned}$$

Despite the indications for a dispersed micelle corona, a near-hard-sphere potential is expected as a result of entropic repulsions.<sup>8</sup>

The scattering function can thus be expressed in an analytical form with only three parameters, the hard-sphere volume fraction,  $\phi$ , and two radii characterizing the micelles: the micelle core radius,  $R_c$ , and the hard-sphere interaction radius,  $R_{hs}$ . Very good fits (see Figure 6b for representative examples) to the experimental scattering patterns have been obtained from the combination of eqs 5, 4, and 6, thus allowing the calculation of  $R_c$ ,  $R_{hs}$ , and  $\phi$  at different block copolymer concentrations and solution temperatures.

Values for  $R_c$  and  $R_{hs}$  in EO<sub>37</sub>PO<sub>58</sub>EO<sub>37</sub>-formamide solutions are presented in Figure 7, b and c, respectively, plotted as a function of temperature for high (8, 14, and 20 wt %) block copolymer concentrations. The main trend discerned is that of an increase in the radii with increasing temperature.  $R_c$  goes from 39 Å at 30 °C to 47 Å at 60 °C, a 20% increase.  $R_{hs}$  increases by 15% (from 57 to 66 Å) over the same temperature range. This increase in the micelle radii reflects the changes in the number of block copolymers participating in a micelle at different temperatures but, as discussed below, is also affected by the degree of solvation in the micelle corona and core. Another important observation from Figure 7b,c concerns the independence of the radii to the block copolymer concentration (in the range 8–20%). Both these trends are consistent with the behavior of PEO-PPO micelles in water.<sup>8</sup>

The PEO-PPO micelle radii obtained in formamide are about 20% lower than the corresponding radii in water. The formation in formamide and in other non-aqueous polar solvents of micelles that are smaller than those in water is generally observed in surfactant systems.<sup>19,25</sup> Small micelles, with a large part of the surfactant hydrocarbon chain in contact with the solvent, are very unfavorable in water because the interfacial tension between water and hydrocarbon is high. However, the interfacial tension in nonaqueous



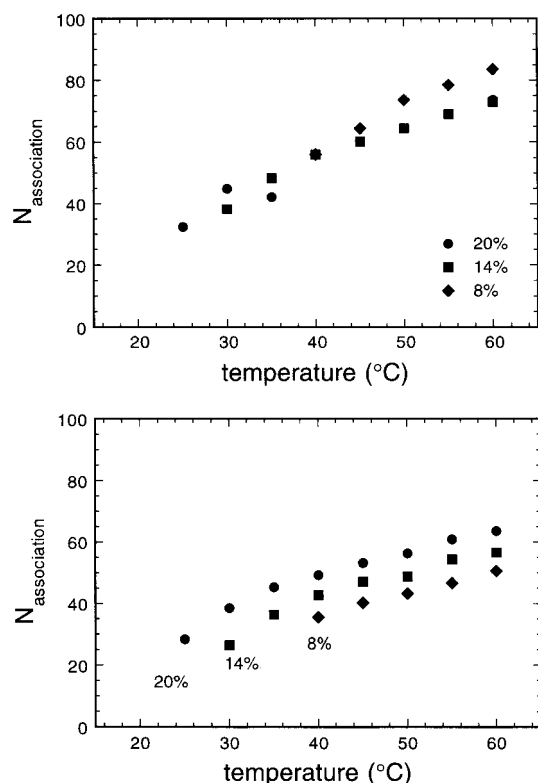


**Figure 8.** Micelle association number,  $N_{\text{association}}$ , obtained (top) on the basis of the micelle core radius,  $R_c$  (eq 8), and (bottom) from the micelle volume fraction,  $\phi$ , and the hard-sphere interaction distance,  $R_{\text{hs}}$  (eq 9), plotted as a function of temperature for different block copolymer concentrations (8, 14, and 20 wt %).

polar solvents and hydrocarbon is smaller, and thus, from this point of view, smaller micelles are less energetically unfavorable.<sup>19</sup>

**Micelle Association Number.** From the micelle core radius values obtained above, and with the assumption that the micelle core consists of all the PPO segments of the block copolymers which participate in one micelle, and of only the PPO blocks (i.e., there is no solvent or PEO present in the core), we can estimate the number of block copolymers per micelle,  $N_{\text{association}}$ , as follows:

$$N_{\text{association}} = 4\pi R_c^3 / 3mv_{\text{PO}} \quad (8)$$

where  $n$  is the number of PPO segments per block copolymer (for Pluronic P105  $n = 58$ ) and  $v_{\text{PO}}$  is the molecular volume of one PPO segment ( $v_{\text{PO}} = 94.5 \text{ \AA}^3$ ).

Values for  $N_{\text{association}}$  are presented in Figure 8a as a function of temperature for different block copolymer concentrations.  $N_{\text{association}}$  increases linearly with temperature (in the range 25–60 °C) from 35 to almost 80.  $N_{\text{association}}$  values overlap for 14 and 20% polymer, but the 8% micelles show a  $N_{\text{association}}$  higher by about 5–10, reflecting the small difference in  $R_c$  between the 8% micelles and the 14 and 20% micelles (see Figure 7b). The  $N_{\text{association}}$  values in the case of formamide are on the same order of magnitude but smaller than those observed when water is the solvent. A  $N_{\text{association}}$  value of 60 leads to a “molecular weight” of about 400 000 for one micelle.

The assumption invoked in eq 8 is that of strong segregation between the PEO and PPO blocks and between the PPO blocks and the solvent. Such strong segregation is probably not the case, and we cannot

exclude the presence of PEO segments in the micelle core and/or the presence of PPO segments in the corona and/or the presence of solvent in the core. Nevertheless, eq 8 will still hold, as long as the amount of PEO in the core is comparable to the amount of PPO in the corona, and there is no solvent present in the core. Since formamide is a better solvent than water for both PEO and PPO segments, the presence of formamide into the PPO core of the micelle cannot be neglected. In this case, eq 8 would lead to an overestimation of  $N_{\text{association}}$ .

An alternative method to estimate  $N_{\text{association}}$  in the  $\text{EO}_{37}\text{PO}_{58}\text{EO}_{37}$ –formamide system, without the assumption discussed above, is to use the micelle volume fraction  $\phi$  and the micelle hard-sphere interaction radius  $R_{\text{hs}}$  obtained from the SANS data fitting as described above. In this case,  $N_{\text{association}}$  can be expressed as a function of  $R_{\text{hs}}$  and  $\phi$ :

$$N_{\text{association}} = (C - C_{\text{free}})4\pi R_{\text{hs}}^3 / (3\phi v_p) \quad (9)$$

where  $C$  is the block copolymer concentration and  $v_p$  is the volume of one P105 block copolymer molecule ( $v_p = 2mv_{\text{EO}} + mv_{\text{PO}} = 10\,940 \text{ \AA}^3$ ). We assume that the concentration of free block copolymer (unimer),  $C_{\text{free}}$ , is equal to the cmc at the same temperature and that the free block copolymer concentration remains constant over the polymer concentration range 8–20%. The cmc values we used for this calculation are those shown in Figure 5.

Values for  $N_{\text{association}}$  calculated using eq 9 are plotted in Figure 8b. The same trend as in Figure 8a of increasing  $N_{\text{association}}$  with temperature is also observed in Figure 8b where  $N_{\text{association}}$  almost doubles in the temperature range 25–60 °C. Contrary to Figure 8a, the data of Figure 8b show a consistent trend of increasing  $N_{\text{association}}$  with increasing block copolymer concentration at a given temperature. Compared to the  $N_{\text{association}}$  values obtained on the basis of the micelle core radius (eq 8), the  $N_{\text{association}}$  values obtained from the micelle volume fraction and the hard-sphere interaction distance (eq 9) are lower. Given that  $R_c$ ,  $R_{\text{hs}}$ , and  $\phi$  are the results of fits (with some degree of uncertainty), the “true”  $N_{\text{association}}$  is probably intermediate to that shown in Figure 8a,b. The discrepancy between the two data sets is a clear indication that the micelle core is not “dry” but contains some solvent and/or PEO.

The  $N_{\text{association}}$  values estimated above can be compared to those obtained<sup>31</sup> in the micellar cubic structure, at much higher block copolymer concentration (40%), using a different experimental technique (small-angle X-ray scattering, SAXS) and different assumptions. From SAXS we obtained the cubic cell lattice parameter,  $a$ . From the number of micelles,  $N$ , per unit cell and the volume of the micellar cubic unit cell,  $a^3$ , we obtained the volume per micelle ( $a^3/N$ ), and then, given the polymer volume fraction,  $\phi_p$ , and the volume per block copolymer molecule,  $v_p$ , we estimated the number of block copolymer molecules per micelle as  $(\phi_p a^3)/(Nv_p)$ . This value in formamide at 30 °C was 77, whereas that in water was much higher: 157.<sup>31</sup>  $N_{\text{association}} = 77$  is higher than the values shown in Figure 8 but is closer to the values obtained from eq 8.

**Micelle Degree of Solvation.** From the above analysis it becomes clear that the solvent which is present within the volume occupied by a block copolymer micelle merits explicit consideration. If we consider the hard-sphere interaction radius,  $R_{\text{hs}}$ , to indicate the



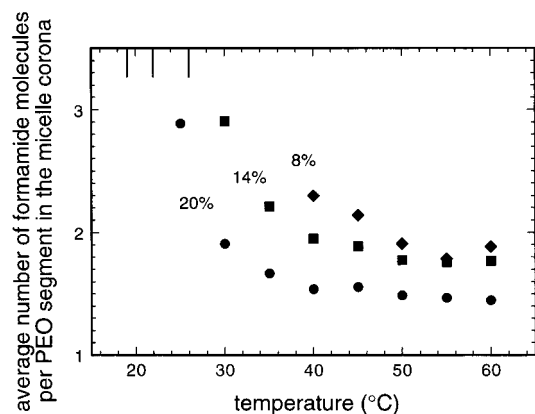


**Figure 9.** Solvation number (formamide molecules per PEO segment) in the micelle corona plotted as a function of temperature for different block copolymer concentrations (8, 14, and 20 wt %). The vertical lines on the upper *X*-axis indicate the cmc of the respective block copolymer concentrations.

extent into the solution of the PEO blocks of the block copolymers that participate in a given micelle, then we can calculate the volume of the micelle corona as that between two concentric spheres defined by  $R_{hs}$  and the micelle core radius,  $R_c$ . From the volume of the micelle corona we can estimate the average number of formamide molecules per PEO segment,  $N_{solvation,PEO}$ :

$$N_{solvation,PEO} = [4\pi(R_{hs}^3 - R_c^3)/3 - N_{association}2mv_{EO}]/(v_{fm}N_{association}2m) \quad (10)$$

where  $m$  is the number of segments per PEO block (for Pluronic P105  $m = 37$ ),  $v_{EO}$  is the molecular volume of one PEO segment ( $v_{EO} = 73 \text{ \AA}^3$ ), and  $v_{fm}$  is the molecular volume of one formamide molecule ( $v_{fm} = 66 \text{ \AA}^3$ ). In addition to the  $N_{solvation,PEO}$ , we can estimate the volume fraction of PEO in the corona,  $\Phi_{PEO,corona}$ :

$$\Phi_{PEO,corona} = (2nN_{association}v_{EO})/[4\pi(R_{hs}^3 - R_c^3)/3] \quad (11)$$

The  $N_{solvation,PEO}$  and  $\Phi_{PEO,corona}$  were calculated using the  $N_{association}$  values obtained from eq 10 and the  $R_{hs}$  and  $R_c$  values obtained from the SANS fits. Values for  $N_{solvation,PEO}$  are plotted in Figure 9 as a function of temperature for different block copolymer concentrations. The average number of formamide molecules per PEO segment decreases with the increase of temperature from a high value of 3 down to 1.5–2. This decrease indicates that formamide becomes progressively less good solvent for PEO. It is notable that  $N_{solvation,PEO}$  is higher at the lower block copolymer concentration (8%). This suggests a looser micelle structure at these conditions and is related to a lower  $N_{association}$  (as seen in Figure 8b) at a time that the micelle radii appear independent of the block copolymer concentration (Figure 7b,c). The above are in agreement with observations of the micelle structure in aqueous solutions.<sup>37</sup> The  $\Phi_{PEO,corona}$  values corresponding to the data of Figure 9 are approximately constant over the temperature range investigated, at the levels of 0.85, 0.75, and 0.65 for 20, 14, and 8% block copolymer, respectively.

In the same manner in which we calculated  $N_{solvation,PEO}$  and  $\Phi_{PEO,corona}$ , we can estimate  $N_{solvation,PPO}$  and

$$\Phi_{PPO,core}:$$

$$N_{solvation,PPO} = [4\pi R_c^3/3 - N_{association}mv_{PO}]/(v_{fm}N_{association}m) \quad (12)$$

$$\Phi_{PPO,core} = (mN_{association}v_{PO})/[4\pi R_c^3/3] \quad (13)$$

Compared to  $N_{solvation,PEO}$ , the average number of formamide molecules per PPO segment is not affected much by the temperature. The trend of higher solvation number for the lower block copolymer concentration also holds for  $N_{solvation,PPO}$ . While the  $R_{hs}$  and  $R_c$  resulting from the SANS fits remain almost independent of concentration at different temperatures, the hard-sphere volume fraction is higher at low concentration. This indicates looser block copolymer assemblies at low concentration and higher solvent content into the micelle structure. However, due to the presence of the deuterated solvent into the hydrogenated block copolymer micelles, the contrast between the block copolymer and the solvent becomes weaker, and the sensitivity and accuracy of the SANS data fits are reduced. For this reason we only discuss the trends above and will not go into detail presenting the  $N_{solvation,PPO}$  and  $\Phi_{PPO,core}$  values obtained from eqs 12 and 13.

## Summary

The micelle formation and structure of a poly(ethylene oxide)–poly(propylene oxide)–poly(ethylene oxide) (PEO–PPO–PEO) block copolymer (Pluronic P105: EO<sub>37</sub>PO<sub>58</sub>EO<sub>37</sub>) in formamide was investigated as a function of block copolymer concentration and temperature using small-angle neutron scattering (SANS). The PEO–PPO–PEO block copolymers form micelles in formamide upon increasing the temperature, indicating an endothermic micellization, similar to the PEO–PPO–PEO micellization in water. However, the enthalpy and entropy of micellization in formamide are about 3 times smaller than the respective quantities in water. Also, the concentration and temperature at which micelles form are higher in formamide than in water.

The radius of gyration of the unimers and the core radius and hard-sphere interaction radius of the spherical micelles were obtained by fitting appropriate models of the form and structure factor to the SANS scattering patterns. The unimer radius was found higher in formamide compared to that in water. The micelle radii were in the range 40–60 Å. They exhibited a strong increase with increasing temperature but did not depend on the block copolymer concentration. The number of block copolymer molecules that participate in each micelle and the degree of solvation of the micelle were estimated using the different radii on the basis of simple geometrical models for the spherical micelles. The association number was in the range 40–60 and increased with temperature. The amount of solvent in the micelle corona decreased with increasing temperature up to 15 °C above the cmc and then remained constant (for the temperature range examined) at a value of about 1.5 solvent molecules per ethylene oxide segment. The presence of solvent in the micelle core is supported by our data. The amount of solvent in the micelles is higher at lower block copolymer concentrations, indicating a loose structure.

The higher cmc and cmt, lower enthalpy of micellization, larger unimer radius of gyration, lower micelle radii, and lower association number that were observed

in formamide compared to those observed in aqueous solutions all suggest that formamide is a better solvent than water for the PEO-PPO-PEO block copolymers. The trends in the above parameters observed with increasing temperature are the same in formamide and water, suggesting a common mechanism of block copolymer segregation in the two solvents.

**Acknowledgment.** This work was partially supported by the Petroleum Research Fund, administered by the American Chemical Society (ACS-PRF# 33408-G7), and by the National Science Foundation (CTS-9875848). We acknowledge the support of the National Institute of Standards and Technology (NIST), U.S. Department of Commerce, in providing the neutron research facilities used in this work. This material is based upon activities supported by the National Science Foundation under Agreement DMR-9423101. We are grateful to Dr. Tania M. Slawacki and Dr. Paul D. Butler at NIST for valuable assistance with the SANS data acquisition and analysis.

## References and Notes

- (1) Evans, D. F.; Wennerström, H. *The Colloidal Domain: Where Physics, Chemistry, Biology, and Technology Meet*, 2nd ed., VCH Publishers: New York, 1999.
- (2) Lindman, B.; Wennerström, H. *Top. Curr. Chem.* **1980**, *87*, 1–83. Laughlin, R. G. *The Aqueous Phase Behavior of Surfactants*; Academic Press: London, 1994.
- (3) Alexandridis, P.; Hatton, T. A. In *Polymeric Materials Encyclopedia*; Salamone, J. C., Editor-in-Chief; CRC Press: Boca Raton, FL, 1996; pp 743–754.
- (4) Alexandridis, P.; Spontak, R. J. *Curr. Opin. Colloid Interface Sci.* **1999**, *4*, 130–139.
- (5) Alexandridis, P.; Hatton, T. A. *Colloids Surf. A* **1995**, *96*, 1–46.
- (6) Alexandridis, P. *Curr. Opin. Colloid Interface Sci.* **1997**, *2*, 478–489.
- (7) Alexandridis, P.; Holzwarth, J. F.; Hatton, T. A. *Macromolecules* **1994**, *27*, 2414–2425.
- (8) Mortensen, K. *J. Phys.: Condens. Matter* **1996**, *8*, A103–A124.
- (9) Alexandridis, P. *Curr. Opin. Colloid Interface Sci.* **1996**, *1*, 490–501.
- (10) Yang, L.; Alexandridis, P. *ACS Symp. Ser.* **2000**, *752*, in press.
- (11) Wanka, G.; Hoffmann, H.; Ulbricht, W. *Macromolecules* **1994**, *27*, 4145–4159.
- (12) Alexandridis, P.; Zhou, D.; Khan, A. *Langmuir* **1996**, *12*, 2690–2700.
- (13) Alexandridis, P.; Olsson, U.; Lindman, B. *Langmuir* **1998**, *14*, 2627–2638.
- (14) Holmqvist, P.; Alexandridis, P.; Lindman, B. *J. Phys. Chem. B* **1998**, *102*, 1149–1158.
- (15) Alexandridis, P.; Andersson, K. *J. Phys. Chem. B* **1997**, *101*, 8103–8111.
- (16) Cheng, Y.; Jolicœur, C. *Macromolecules* **1995**, *28*, 2665–2672.
- (17) Alexandridis, P.; Athanassiou, V.; Hatton, T. A. *Langmuir* **1995**, *11*, 2442–2450.
- (18) Alexandridis, P.; Holzwarth, J. F. *Langmuir* **1997**, *13*, 6074–6082.
- (19) Sjöberg, M.; Wårnheim, T. *Surfactant Sci. Ser.* **1997**, *67*, 179–205.
- (20) Evans, D. F. *Langmuir* **1988**, *4*, 3–12.
- (21) Zana, R. *Colloids Surf. A* **1997**, *123–124*, 27–35.
- (22) Wårnheim, T. *Curr. Opin. Colloid Interface Sci.* **1997**, *2*, 472–477.
- (23) Couper, A.; Gladden, G. P.; Ingram, B. T. *Faraday Discuss. Chem. Soc.* **1975**, *59*, 63–75.
- (24) Jonströmer, M.; Sjöberg, M.; Wårnheim, T. *J. Phys. Chem.* **1990**, *94*, 7449–7555.
- (25) Olofsson, G. *J. Chem. Soc., Faraday Trans.* **1991**, *87*, 3037–3042.
- (26) Schubert, K. V.; Busse, G.; Strej, R.; Kahlweit, M. *J. Phys. Chem.* **1993**, *97*, 248–254.
- (27) Ceglie, A.; Colafemmina, G.; Della Monica, M.; Olsson, U.; Jönsson, B. *Langmuir* **1993**, *9*, 1449–1455.
- (28) Perche, T.; Auvray, X.; Petipas, C.; Anthore, R.; Rico-Lattes, I.; Lattes, A. *Langmuir* **1997**, *13*, 1475–1480.
- (29) Samii, A. A.; Karlström, G.; Lindman, B. *Langmuir* **1991**, *7*, 1067–1071.
- (30) Imhof, A.; Pine, D. J. *Nature* **1997**, *389*, 948–951.
- (31) Alexandridis, P. *Macromolecules* **1998**, *31*, 6935–6942.
- (32) Alexandridis, P.; Nivaggioli, T.; Hatton, T. A. *Langmuir* **1995**, *11*, 1468–1476.
- (33) Kositzka, M.; Bohne, C.; Alexandridis, P.; Hatton, T. A.; Holzwarth, J. F. *Langmuir* **1999**, *15*, 322–325.
- (34) Higgins, J. S.; Benoit, H. C. *Polymers and Neutron Scattering*; Oxford University Press Inc.: New York, 1996.
- (35) Mortensen, K.; Pedersen, J. S. *Macromolecules* **1993**, *26*, 805–812.
- (36) Wu, G.; Chu, B.; Schneider, D. K. *J. Phys. Chem.* **1995**, *99*, 5094–5101.
- (37) Goldmints, I.; von Gottberg, F. K.; Smith, K. A.; Hatton, T. A. *Langmuir* **1997**, *13*, 3659–3664.
- (38) Liu, Y.; Chen, S.-H.; Huang, J. S. *Macromolecules* **1998**, *31*, 2236–2244.
- (39) Jain, N. J.; Aswal, V. K.; Goyal, P. S.; Bahadur, P. *J. Phys. Chem. B* **1998**, *102*, 8452–8458.
- (40) Svensson, B.; Olsson, U.; Alexandridis, P.; Mortensen, K. *Macromolecules* **1999**, *32*, 6725–6733.
- (41) Mortensen, K.; Brown, W.; Norden, B. *Phys. Rev. Lett.* **1992**, *68*, 2340–2343.
- (42) Prud'homme, R. K.; Wu, G.; Schneider, D. K. *Langmuir* **1996**, *12*, 4651–4659.
- (43) Slawacki, T. M.; Glinka, C. J.; Hammouda, B. *Phys. Rev. E* **1998**, *58*, R4084–R4087.
- (44) Molino, F. R.; Berret, J. F.; Porte, G.; Diat, O.; Lindner, P. *Eur. Phys. J. B* **1998**, *3*, 59–72.
- (45) Yang, L.; Slawacki, T. M.; Alexandridis, P. *Macromolecules* **2000**, submitted.
- (46) Schmidt, G.; Richtering, W.; Lindner, P.; Alexandridis, P. *Macromolecules* **1998**, *31*, 2293–2298.
- (47) Alexandridis, P.; Ivanova, R.; Lindman, B. *Langmuir* **2000**, *16*, in press.
- (48) Svensson, M.; Alexandridis, P.; Linse, P. *Macromolecules* **1999**, *32*, 637–645.

MA990862O